EEET ECOLOGICAL ENGINEERING & ENVIRONMENTAL TECHNOLOGY

Ecological Engineering & Environmental Technology, 2025, 26(12), 124–138
https://doi.org/10.12912/27197050/214044
ISSN 2719–7050, License CC-BY 4.0

Received: 2025.10.27
Accepted: 2025.11.15
Published: 2025.12.01

Comparative assessment of soil greenhouse gas fluxes (carbon dioxide and methane) and climate effects across wetland types in South Bali, Indonesia

I Gusti Ngurah Putu Dharmayasa[1*], Kenny Christovorus Manek[1], Putu Adi Suryaputrawan[1], I Putu Sugiana[2], Romanee Thongdara[3]

[1] Department of Civil Engineering, Faculty of Engineering and Informatics, Universitas Pendidikan Nasional, Denpasar 80224, Indonesia
[2] Department of Aquatic Resources Management, Faculty of Agriculture, Science and Technology, Universitas Warmadewa, Denpasar 80235, Bali, Indonesia
[3] Department of Civil and Environmental Engineering, Mahidol University, Nakhon Pathom 73170, Thailand
* Corresponding author's e-mail: ngurahdharmayasa@undiknas.ac.id

ABSTRACT

Wetlands help keep the Earth's carbon in check. They do this by storing carbon over long periods and releasing greenhouse gases. In Indonesia, even though land use is changing quickly, there hasn't been much research comparing different wetland types. This study focused on six wetlands in South Bali, ranging from healthy and degraded mangroves to marshes, rice fields, mudflats, and abandoned aquaculture ponds. Researchers collected data on soil traits like organic carbon content, moisture, pH, bulk density, and texture. During the dry season, we measured fluxes of carbon dioxide (CO_2) and methane (CH_4) using static closed chambers and gas chromatography, then calculated its climate impact in CO_2-equivalent terms. The results varied across sites: degraded mangroves had the highest emissions, while mudflats and rice paddies absorbed more carbon than they released. CO_2 emissions tended to be higher in more acidic soils, but CH_4 wasn't as clearly linked to soil features. Overall, wetlands in poor condition were shown to contribute more to warming, while healthy or managed ones offered climate benefits. These findings support efforts to conserve undisturbed wetlands and restore damaged ones to help tackle climate change more naturally.

Keywords: greenhouse gases, carbon dioxide, methane, static closed chambers.

INTRODUCTION

While wetlands cover only a sliver of the Earth's land area, their role in the global carbon cycle is far more substantial than their size suggests. These ecosystems trap large volumes of carbon in waterlogged soils where the lack of oxygen slows decomposition. In doing so, they function as long-term carbon sinks but also release greenhouse gases such as carbon dioxide (CO_2), methane (CH_4), and nitrous oxide (N_2O), as microbes break down organic material (Kauffman et al., 2020; Villa and Bernal, 2018). The mix of gases released varies depending on environmental conditions and determines whether a wetland warms or cools the atmosphere overall. This delicate balance is affected by several factors, including water levels, salinity, redox state, available carbon sources, and human-related changes (Kristensen et al., 2008; Saunois et al., 2016; Alongi, 2018).

Each wetland type behaves differently in this context. Take rice paddies, for instance – they're man-made, flooded fields that are globally important for food production but also major sources of CH_4. This is mainly due to constant water saturation, which favors methanogenic microbes, though local practices like irrigation and organic inputs influence the scale of emissions (Gupta et al., 2021). Mangroves, on the other hand, are

among the most efficient carbon-storing ecosystems, especially underground. But they are not uniform: intact mangroves with strong root activity tend to limit methane, whereas degraded ones where hydrology is altered or canopy is lost may emit more CO_2 and CH_4 (Thibodeau and Nickerson, 1986; Donato et al., 2011; Romero-Uribe et al., 2021). Abandoned aquaculture sites add another layer of complexity, as changes in sediment, nutrients, and water levels can flip them between being carbon sources and sinks (Castillo et al., 2017). In the tropics, where temperatures are high and rainfall are seasonal, these dynamics are intensified. Rain and heat speed up microbial activity, while salinity and redox fluctuations change which gases are released (Chen et al., 2014; Rosentreter et al., 2018; Cameron et al., 2019).

In Indonesia, much remains unknown about these processes. The country is home to widespread rice cultivation, expanding aquaculture, and vulnerable mangrove forests, often side-by-side in crowded coastal zones. Despite this, very few studies have directly compared greenhouse gas emissions across these ecosystems, especially using measurements that also consider soil features like organic carbon content, density, moisture, and pH. This gap limits our understanding of how management and environmental conditions interact, and makes it harder to assess trade-offs between farming, aquaculture, and ecosystem services. It also holds back efforts to create reliable data for climate policy. For example, in degraded black mangroves, methane tends to spike in the rainy season due to warm, salty, and oxygen-poor conditions. CO_2, in contrast, often rises during dry periods when the soil is more aerated. NO_2 doesn't show clear seasonal trends but responds more erratically to nitrogen cycling (Romero-Uribe et al., 2021). These patterns underscore how land use and water management can rapidly reshape a wetland's climate role.

South Bali is well suited to explore these questions. Earlier studies here mostly focused on mangroves (Sugiana et al., 2023; Sugiana et al., 2024; Dharmayasa et al., 2025), but the region hosts a variety of wetlands including rice paddies, healthy and degraded mangroves, mudflats, and abandoned ponds all within short distances of one another. This landscape, shaped by monsoon rains, salinity shifts, and tourism-driven land pressures, offers a rare chance to examine how different wetland types behave under similar climate conditions. Yet, there has been little coordinated research comparing their carbon emissions.

This study addresses that gap by examining greenhouse gas emissions from soils across six wetland types in South Bali: dead mangrove, mudflat, marshland, rice field, abandoned aquaculture, and healthy mangrove. We measured both CO_2 and CH_4 concentrations and fluxes, related them to soil properties like carbon content, density, moisture, and pH, and analyzed short-term gas patterns during incubation. These values were then converted into CO_2-equivalents to estimate the climate impact of each site. Our aim is to better understand what drives carbon cycling in these systems, and how human activity influences whether they act as warming sources or cooling sinks. The findings can help guide conservation, sustainable land use, and policy-making in Indonesia's vulnerable coastal zones. They also offer real-world data to improve emission estimates used in regional and global carbon reporting (Donato et al., 2011; Kauffman and Donato, 2012; IPCC, 2021).

METHOD

Site description

This research took place in South Bali, where most of the sampling locations were within 2.5 kilometers of the coast, spanning coordinates from 8°40′51.61″S to 8°44′21.55″S and 115°10′22.77″E to 115°15′14.53″E. The study focused on five different types of wetlands: mangroves, aquaculture ponds, mudflats, marshlands, and rice paddies. For the mangrove category, two distinct site conditions were selected—one representing healthy, densely vegetated areas and the other featuring degraded zones with widespread tree dieback. The aquaculture site included ponds that had been unused for over three years, allowing tidal seawater to flow into the system naturally. The mudflat site was located next to mangrove forests and experienced regular tidal flooding. The marshland area was dominated by shrubs, remained waterlogged during the rainy season, and was crisscrossed by small drainage channels. Finally, the rice field site reflected an actively cultivated paddy where rice seedlings had been planted roughly a week before data collection. Figure 1 provides an overview of the site layout and the specific characteristics of each wetland type.

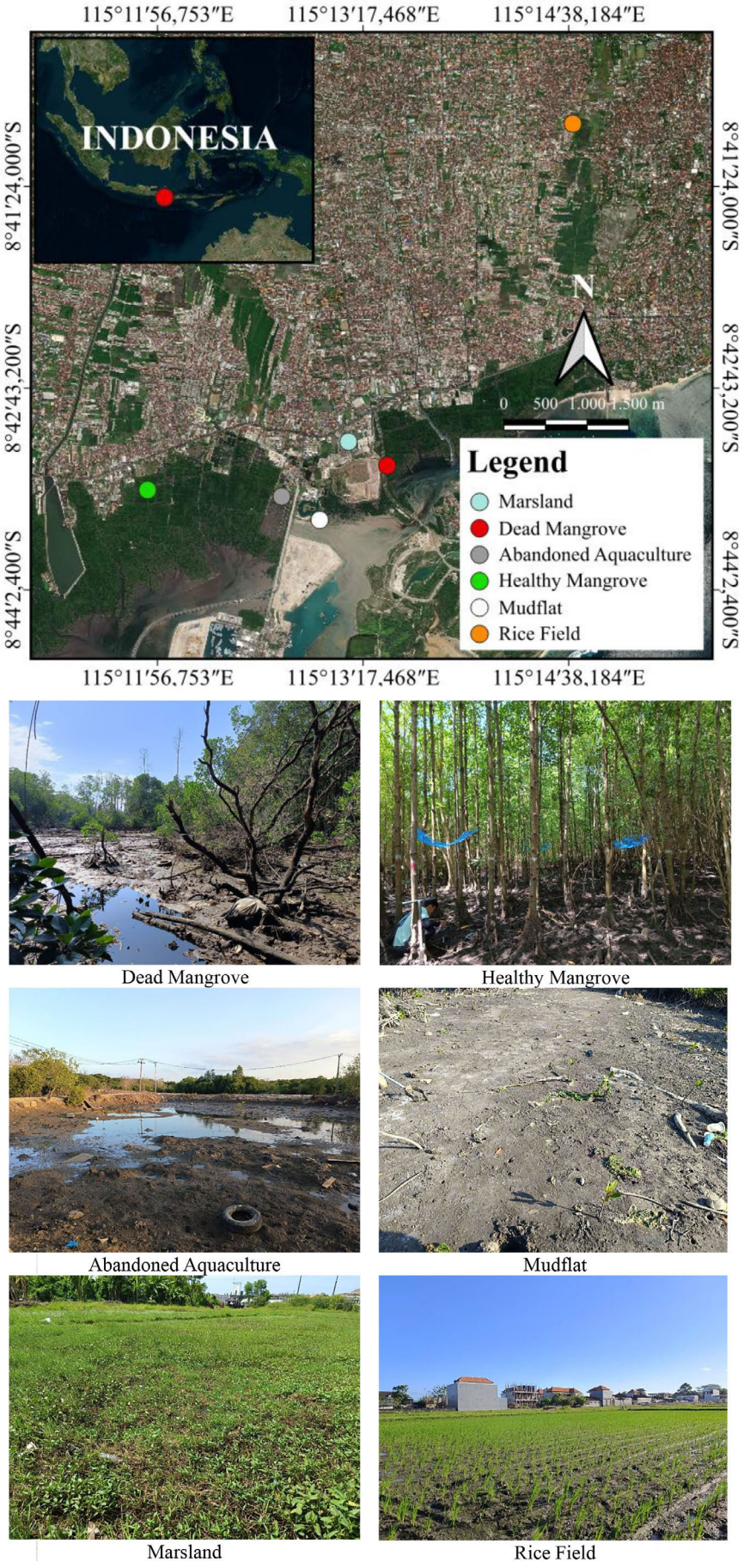

Figure 1. Research location map and its condition in South Bali

Soil data collection

Soil sampling was carried out using a manual auger with a 5 cm diameter, collecting cores from the surface down to a depth of 100 cm. Field pH measurements were immediately taken using a Lutron 212 pH meter. Each core was then thoroughly mixed, and a 200 g portion was transferred into plastic bags for laboratory analysis. To determine gravimetric water content, samples were oven-dried at 70 °C until reaching a constant weight, typically within 48 hours. For bulk density analysis, a 100 g subsample was further dried at 105 °C. The remaining soil material was processed for texture assessment. Coarse particles including gravel (>2 mm) and sand (1.1 mm to 75 μm) were separated through dry sieving. Finer fractions, consisting of silt and clay, were quantified using the pipette sedimentation method. Total organic carbon (TOC) content was assessed by the loss-on-ignition (LOI) method, where dried samples were combusted at 550 °C following the procedure described by Chen et al. (2016). All processes are illustrated in Figure 2.

Gas sample collection and carbon fluxes calculation

Gas sampling was conducted using 10 mL syringes, following a chamber incubation approach adapted from Chen et al. (2014). Cylindrical chambers (17 cm in diameter, 18.5 cm in height, volume approximately 4200 cm^3) were gently inserted about 2 cm into the sediment surface at locations without visible burrows

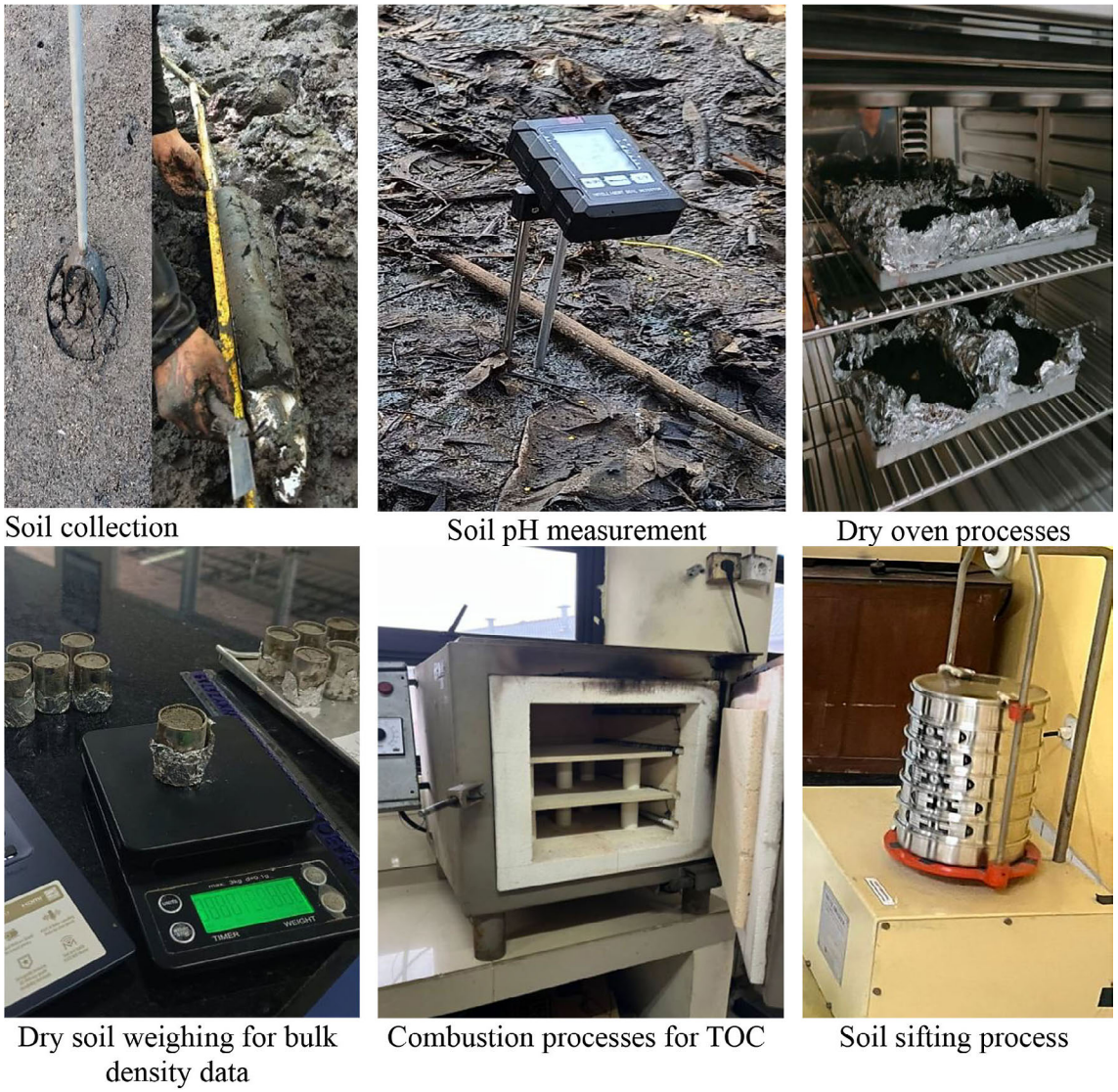

Figure 2. Illustration for soil data collection

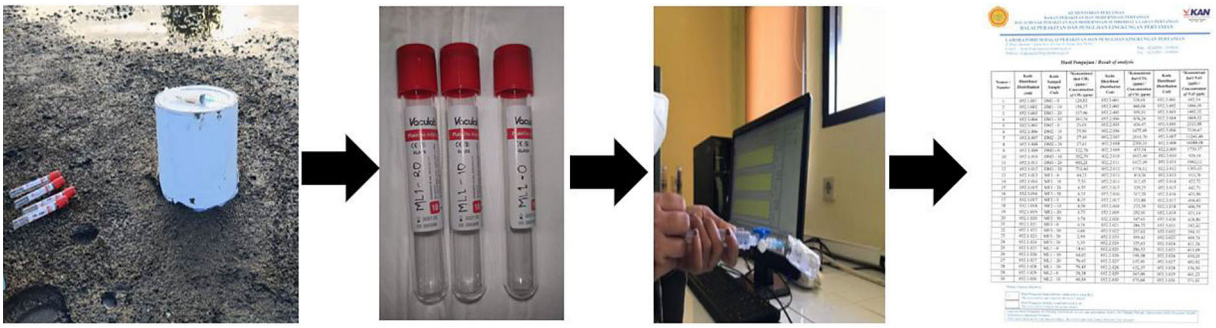

Gas sample collection | Gas Sample collected on vacutainer tube | Gas sample injection process in GCMS | Laboratory results

Figure 3. Documentation of gas incubation processes using static chamber and laboratory processes

or plant debris (see Figure 3). Each incubation lasted 30 minutes, with gas drawn at four-time intervals: 0, 10, 20, and 30 minutes. Sampling took place in August 2025, corresponding with the height of the dry season. Across six stations, a total of 72 gas samples were collected using three chambers per station, with four gas samples extracted from each chamber. All samples were immediately transferred into 10 mL evacuated glass tubes (vacutainers) for storage and later analysis.

The gas samples were analyzed at the Laboratory of Agricultural Environmental Research, Pati, Central Java, to determine CH_4 and CO_2 concentrations. Measurements were performed using a 450-GC Varian gas chromatograph equipped with a flame ionization detector (FID) and a thermal conductivity detector (TCD). The system was also fitted with a PAL autosampler injector (2 mL) and employed Ar, H_2, He, N_2, and compressed air as carrier gases. Calibration was performed against standard curves, and concentrations were determined by comparing peak areas with the reference standards.

Fluxes of CO_2 and CH_4 were calculated using the equation of Chen et al. (2015):

$$Fm = \frac{V \times \Delta M \times 10^{-6}}{A \times P} \quad (1)$$

where: F_m is the GHG flux (μg m^{-2} h^{-1}), ΔM is the slope of GHG concentration (ppm h^{-1}) obtained from linear regression across incubation intervals (0, 10, 20, 30 min), V is the chamber volume (L), A is the incubated surface area (m^2), and P is the molar volume of an ideal gas (22.414 L mol^{-1}).

Climate impact assessment (warming/cooling effect)

Methane gas fluxes which derived from methane concentration were converted into carbon dioxide equivalents (CO_2-eq) to standardize their warming effect relative to carbon dioxide. The conversion followed the equation of Chen et al. (2015), which multiplies flux values by the molecular weight of the gas and its global warming potential (GWP) over a 100-year time horizon (Figure 4). The equation is expressed as:

$$Fe = Fm \times M \times GMP \quad (2)$$

where: F_e is the warming effect expressed as CO_2-equivalent (g CO_2 m^{-2} h^{-1}), F_m is the GHG flux (mol m^{-2} h^{-1}), M is the molecular weight of the gas (CH_4: 16.04 g mol^{-1}), and GWP is the global warming potential constant (CH_4 = 29.8, N_2O = 273) based on IPCC (2021).

Statistical analysis

All datasets (n = 18; three replicates from six wetland types) were examined for normality using the Shapiro–Wilk test. Since the environmental variables and greenhouse gas flux data did not meet the assumptions of normality ($p < 0.05$), nonparametric methods were employed. Variations in soil characteristics, gas concentrations, and fluxes across wetland types were analyzed using the Kruskal–Wallis test (n = 18), followed by post-hoc pairwise comparisons with Bonferroni adjustments. Correlations between CO_2 and CH_4 fluxes and soil parameters (total organic carbon, bulk density, moisture, and pH) were evaluated

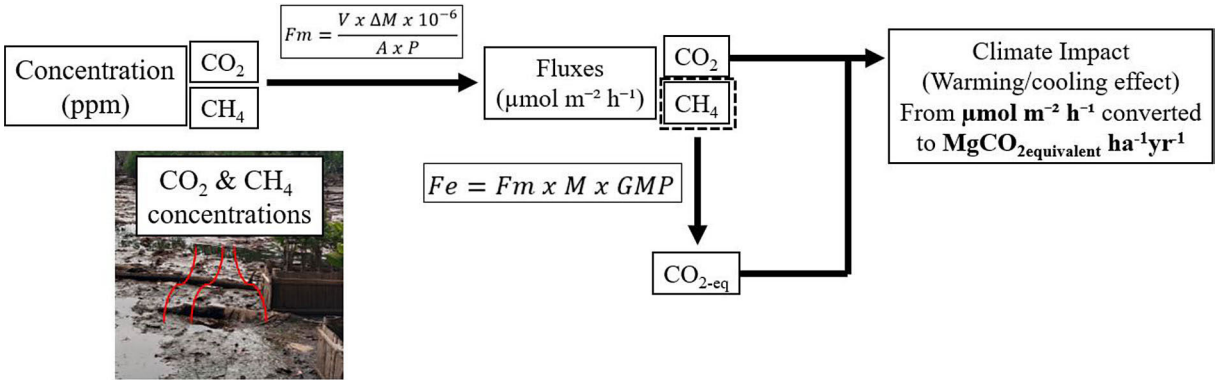

Figure 4. Illustration of convertion from gas concentration to climate impact value

using Spearman's rank correlation. Each chamber (three per site) was treated as an independent replicate. All analyses were conducted at a significance level of $p < 0.05$ using R version 4.0.2.

Results and discussion

Soil properties

Significant variation in several soil parameters was observed across the different wetland types, as indicated by the Kruskal–Walli's test. Total organic carbon (TOC) differed notably among sites ($H = 14.06$; $p = 0.014$), with dead mangrove (DM) showing distinctly elevated levels compared to the rest. In contrast, marshland (ML) and rice field (RF) shared similar TOC values, while mudflat (MF), abandoned aquaculture (TB), and healthy mangrove (HM) formed a group with lower concentrations. Bulk Density also varied significantly ($H = 12.14$; $p = 0.031$), with TB recording the highest density among all sites, whereas DM and ML had the lowest. MF and HM exhibited comparable values, and RF fell between the two groups. A parallel pattern emerged for Water Content ($H = 10.16$; $p = 0.042$), where DM again showed higher values than TB, while ML, HM, and RF displayed intermediate moisture levels. Conversely, no significant differences were found in soil pH across the sites ($H = 10.94$; $p = 0.063$), suggesting generally consistent acidity levels despite minor fluctuations among wetland types (Table 1, 2).

The observed differences in soil properties across wetland types underscore the spatial variability that plays a key role in influencing carbon storage capacity and greenhouse gas behavior. Among all sites, dead mangrove soils recorded the highest levels of TOC, significantly surpassing other wetlands. This pattern likely reflects the build-up of undecomposed organic material following widespread tree mortality—an outcome previously linked to hydrological disruption limiting decomposition rates in degraded mangrove systems (Romero-Uribe et al., 2021; Espinosa-Fuentes et al., 2024). Marshland and rice field soils, by contrast, showed moderate TOC values, which may result from a combination of organic inputs from vegetation and disturbances from agricultural activity. The lowest TOC levels were found in mudflat, abandoned aquaculture, and healthy mangrove sites, which is consistent with studies in other tropical and subtropical regions where mineral-dominated substrates and limited litter stabilization reduce organic matter accumulation (Gamboa-Cutz et al., 2025; Iram et al., 2021).

Bulk Density also varied, with Abandoned Aquaculture sites showing greater compaction and likely accumulation of finer sediments, while Dead Mangrove and Marshland soils were less dense due to their higher organic content and porosity – findings that echo observations from mangrove systems in Mexico and Indonesia (Adhikari et al., 2020; Basheer et al., 2024). A similar trend was found for water content, where dead mangrove soils held more moisture than abandoned aquaculture sites, reinforcing the notion that organic-rich soils tend to retain more water (Gupta et al., 2021; Liu et al., 2017). In contrast, soil pH showed little variation among sites, remaining relatively stable across the wetland types. This aligns with earlier work suggesting that in coastal systems, pH typically fluctuates within a narrow range regardless of vegetation type or land use (Chen et al., 2014; Romero-Uribe et al., 2021). Overall, the findings suggest that TOC, bulk density, and moisture content are highly responsive to site-specific conditions, while pH remains

Table 1. Soil properties of each wetland type (DM = Dead mangrove, MF = Mudflat, ML = Marsland, RF = Rice field, TB = Abandoned aquaculture, HM = Healthy mangrove, 1, 2 & 3 mean the repetition of each wetland type)

Location	Plot	TOC	Bulk density	WC	pH	Soil type
DM	DM1	14.74%	0.48	0.66	6.01	Sandy clay
	DM2	7.57%	0.77	0.48	6.07	Sandy clay
	DM3	6.26%	0.8	0.43	6.18	Sandy clay
MF	MF1	4.67%	1.03	0.34	6.37	Fine sand
	MF2	4.47%	1.07	0.34	6.45	Fine sand
	MF3	6.52%	1.05	0.38	6.28	Fine sand
ML	ML1	6.86%	0.74	0.55	6.43	Sandy clay
	ML2	6.44%	0.84	0.49	6.39	Sandy clay
	ML3	6.57%	0.84	0.47	6.23	Sandy clay
RF	RF1	3.73%	0.99	0.41	6.56	Fine sand
	RF2	6.09%	0.77	0.67	6.48	Fine sand
	RF3	2.80%	1.41	0.28	6.59	Fine sand
TB	TB1	3.73%	1.37	0.30	6.31	Coarse sand
	TB2	2.74%	1.49	0.29	6.35	Coarse sand
	TB3	1.88%	1.34	0.26	6.47	Coarse sand
HM	HM1	0.98%	1.16	0.40	6.36	Fine sand
	HM2	0.97%	1.00	0.43	6.57	Fine sand
	HM3	1.27%	0.94	0.56	6.25	Fine sand

Table 2. Average of soil properties of each wetland and statistical results (Different ^{a,b,c,d} symbols denote that the mean values between wetland types differ significantly according to the Bonferroni statistical test ($p < 0.05$))

Parameter	Station					
	DM	MF	ML	RF	TB	HM
Dominant soil type	Sandy clay	Fine sand	Sandy clay	Fine sand	Coarse sand	Fine sand
Total organic carbon (TOC) %	9.7 ± 4.7^{a}	5.3 ± 1.5^{b}	6.7 ± 0.6^{b}	4.3 ± 1.5^{bc}	3.0 ± 1.0^{cd}	1.0 ± 0.0^{d}
Bulk density (g cm^{-3})	0.7 ± 0.2^{a}	1.0 ± 0.0^{c}	0.8 ± 0.1^{ab}	1.1 ± 0.3^{bc}	1.4 ± 0.1^{c}	1.0 ± 0.1^{bc}
Water content (%)	52.3 ± 12.1^{a}	35.3 ± 2.3^{a}	50.3 ± 4.2^{a}	45.3 ± 19.9^{a}	28.3 ± 2.1^{a}	46.3 ± 8.5^{a}
pH	6.1 ± 0.1^{a}	6.4 ± 0.1^{a}	6.4 ± 0.1^{a}	6.5 ± 0.1^{a}	6.4 ± 0.1^{a}	6.4 ± 0.2^{a}

comparatively consistent – highlighting the central roles of substrate quality, sediment texture, and hydrological regimes in shaping carbon-related processes within these wetlands.

Carbon gas concentration and it's trend during incubation processes

CO_2 concentrations varied significantly across the studied wetland types, as indicated by the Kruskal–Wallis test ($H = 11.87$; $p = 0.037$). The highest mean concentration was recorded at the dead mangrove site (396.6 ± 57.9 ppm), which differed significantly from marshland (257.8 ± 23.3 ppm), rice field (268.4 ± 34.4 ppm), abandoned aquaculture (275.7 ± 36.6 ppm), and healthy mangrove (217.4 ± 22.6 ppm). Although the mudflat site (353.0 ± 65.9 ppm) showed elevated CO_2 levels comparable to Dead Mangrove, the difference was not statistically significant (Figure 5). Marshland and rice field exhibited similar intermediate concentrations and clustered together, while Abandoned Aquaculture grouped closely with rice field and remained distinct from dead mangrove. The healthy mangrove site had the lowest CO_2 levels among all wetlands, forming a clearly separate group.

A similar pattern of variability was observed for CH_4 concentrations, where differences among wetland types were again statistically significant ($H = 13.26$; $p = 0.022$). Dead mangrove stood out with the highest mean CH_4 concentration (90.9 ± 58.8 ppm), significantly exceeding levels recorded at all other sites. Mudflat (18.9 ± 22.0

ppm) and marshland (25.2 ± 5.7 ppm) occupied intermediate positions but were still distinct from rice field (5.3 ± 3.6 ppm), abandoned aquaculture (3.6 ± 0.4 ppm), and healthy mangrove (5.8 ± 0.7 ppm). These three sites exhibited the lowest CH_4 concentrations and did not show significant differences from one another, forming a statistically similar group with minimal variation in methane levels (Figure 5).

Thirty-minute incubation trends in CO_2 concentration revealed distinct patterns across the various wetland types. The dead mangrove site showed a consistently strong increase, particularly in replicates DM2 (+1866.0 ppm) and DM3 (+1350.9 ppm), while DM1 also exhibited a positive trend, though less pronounced (+344.1 ppm). In contrast, the Mudflat site displayed mixed results: MF1 experienced a notable decline (–101.1 ppm), MF2 remained nearly unchanged (–6.9 ppm), and MF3 showed a modest increase (+39.0 ppm). Marshland replicates also varied – ML1 and ML2 recorded decreasing CO_2 levels (–132.3 ppm and –90.9 ppm, respectively), while ML3 showed a sharp rise (+541.5 ppm). Rice field replicates were more uniform, all showing declining CO_2 trends ranging from –43.2 to –61.2 ppm. At the abandoned aquaculture site, CO_2 levels remained remarkably stable across all chambers, with minimal fluctuations (–1.2 to +0.9 ppm). Meanwhile, the healthy mangrove site displayed a consistent upward trend, with increases across all replicates ranging from +56.1 to +210.9 ppm – suggesting a more stable and moderate CO_2 accumulation relative to the more extreme shifts observed in dead mangrove (Figure 6).

Methane (CH_4) concentration trends over the 30-minute incubation period also varied noticeably across wetland types. In the dead mangrove site, two replicates DM1 (+31.7 ppm) and DM2 (+4.4 ppm) showed moderate increases, while DM3 exhibited a dramatic spike in CH_4 concentration (+586.5 ppm), indicating considerable intra-site variability. In contrast, the Mudflat site consistently showed declining trends, with MF1 recording the largest drop (–36.8 ppm), and more modest decreases observed in MF2 (–4.4 ppm) and MF3 (–1.2 ppm). All marshland replicates increased in CH_4 concentration, ranging from +28.8 ppm in ML2 to a peak of +116.2 ppm in ML3, suggesting relatively uniform methane production in this site. Rice field conditions appeared stable, with minor changes between –4.1 and +2.1 ppm across the three chambers. Similar stability was observed in the abandoned aquaculture site, where CH_4 levels remained nearly unchanged (–1.1 to +0.8 ppm). The healthy mangrove site showed consistently small but positive increases in all replicates, with CH_4 rising modestly between +0.5 and +1.9 ppm over the 30-minute period (Figure 7).

Carbon dioxide concentrations varied significantly among the wetland types, with dead mangrove consistently recording the highest average values and standing out distinctly from the other sites. Mudflat sites also showed elevated CO_2 levels, often overlapping with those in dead mangrove, while marshland and rice field formed a middle group with more moderate concentrations. Abandoned aquaculture appeared more aligned with rice field, whereas healthy mangrove had the lowest CO_2 levels, clearly set apart from the rest. These spatial differences were further supported by temporal trends: dead mangrove replicates demonstrated sharp CO_2 increases over the 30-minute

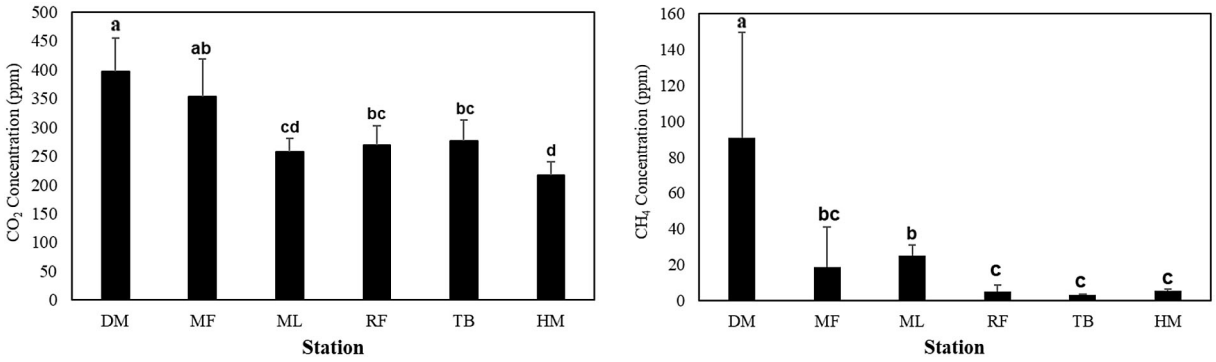

Figure 5. CO_2 concentrations (left) and CH_4 concentrations (right) of each wetland type (DM = dead mangrove, MF = mudflat, ML = marsland, RF = rice field, TB = abandoned aquaculture, HM = healthy mangrove)

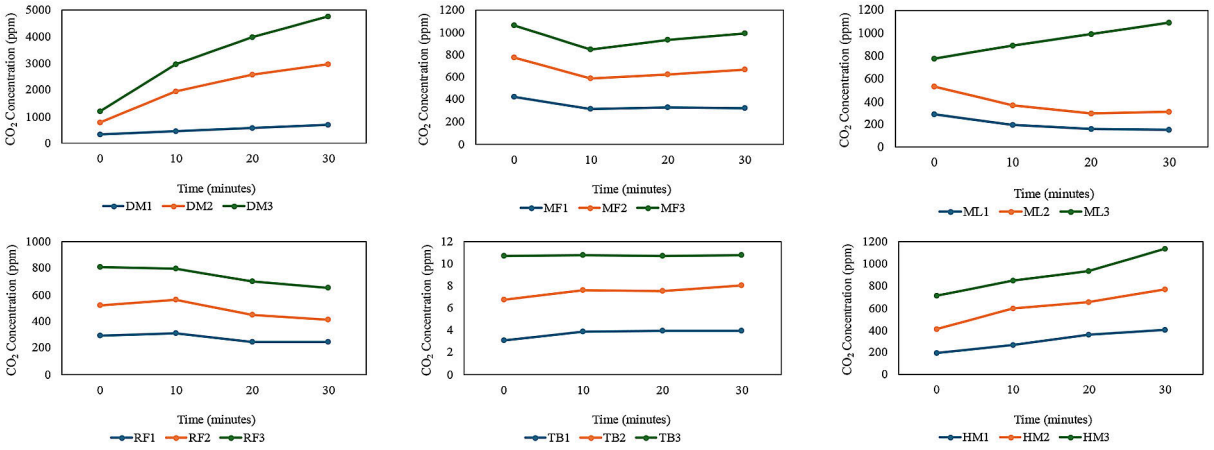

Figure 6. CO_2 concentration trend of each wetland type
(DM = dead mangrove, MF = mudflat, ML = marsland, RF = rice field, TB = abandoned aquaculture, HM = healthy mangrove)

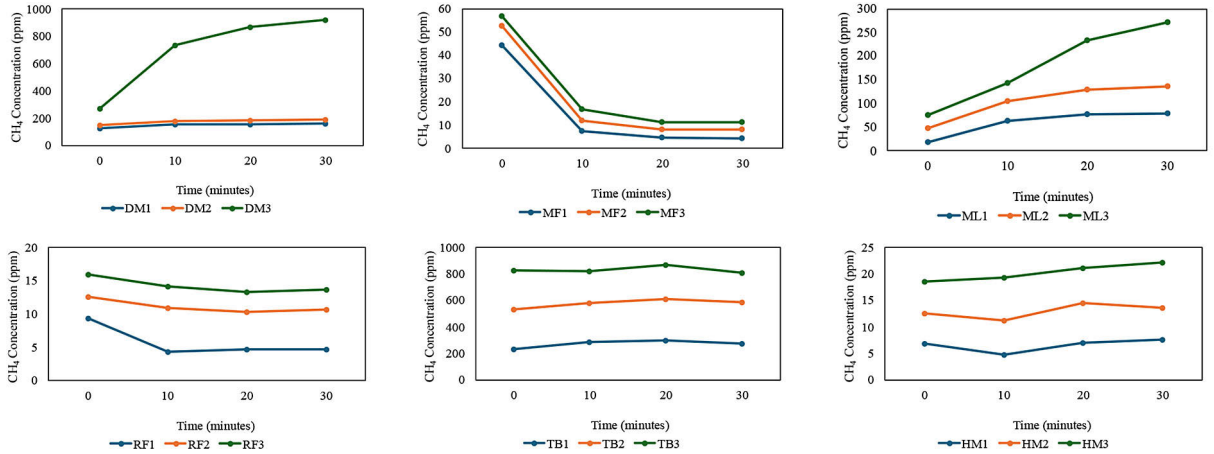

Figure 7. CH_4 concentration trend of each wetland type
(DM = dead mangrove, MF = mudflat, ML = marsland, RF = rice field, TB = abandoned aquaculture, HM = healthy mangrove)

incubation period, while mudflat responses were mixed and marshland trends varied across replicates. In contrast, rice field remained relatively stable or showed slight decreases, and healthy mangrove exhibited a steady but more moderate increase. Notably, the CO_2 concentrations recorded in dead mangrove and mudflat often met or exceeded the current atmospheric average of around 420 ppm (IPCC, 2021), whereas values in healthy mangrove and rice field tended to remain near or below that benchmark. These findings align with earlier research showing that degraded mangrove systems and disturbed soils can accumulate higher levels of CO_2 due to limited gas exchange and reduced plant uptake (Romero-Uribe et al., 2021; Espinosa-Fuentes et al., 2024).

Methane concentrations followed a somewhat similar yet more variable pattern. Once again, dead mangrove registered the highest CH_4 levels and differed significantly from all other wetland types. Marshland and mudflat sites held intermediate concentrations, while rice field, abandoned aquaculture, and healthy mangrove formed a lower group with statistically similar values. During the 30-minute observation period, one dead mangrove replicate exhibited an extreme increase in CH_4, while the others showed more moderate rises. In contrast, all mudflat replicates experienced decreasing trends. Marshland consistently increased across all replicates, whereas rice field and abandoned aquaculture remained nearly unchanged. Healthy mangrove displayed slight but consistent increases. When compared with the

global atmospheric reference level of approximately 1.9 ppm for CH_4 (Saunois et al., 2016), nearly all sites, especially dead mangrove recorded concentrations far exceeding ambient conditions, confirming its role as a significant methane hotspot. This observation supports prior findings that CH_4 emissions in mangroves and wetland soils are highly influenced by redox conditions, substrate availability, and site disturbance (Kristensen et al., 2008; Adhikari et al., 2020; Gamboa-Cutz et al., 2025).

Carbon gas fluxes

The Kruskal–Wallis analysis revealed significant variation in CO_2 fluxes among wetland types ($H = 13.48$, $p = 0.019$). Dead Mangrove exhibited the highest CO_2 emission rates, with a mean flux of 17,057.1 ± 11,116.1 μg m^{-2} h^{-1}, indicating a strong carbon dioxide source to the atmosphere. Post-hoc Bonferroni tests confirmed that CO_2 fluxes at dead mangrove were significantly higher than those at mudflat, rice field, and abandoned aquaculture ($p < 0.05$). Marshland also emitted CO_2, although at a much lower average of 1,542.7 ± 5,474.6 μg m^{-2} h^{-1}, and with large variability among replicates. Healthy mangrove released moderate CO_2 levels (1,068.0 ± 982.1 μg m^{-2} h^{-1}), while abandoned aquaculture sites displayed nearly neutral fluxes (–2.8 ± 753.3 μg m^{-2} h^{-1}). In contrast, mudflat (–173.8 ± 1,004.3 μg m^{-2} h^{-1}) and Rice Field (–808.8 ± 273.2 μg m^{-2} h^{-1}) acted as net carbon sinks, showing negative mean CO_2 fluxes (Figure 8).

Methane (CH_4) fluxes showed a similar but more variable pattern, with statistically significant differences across wetland types ($H = 12.56$, $p = 0.024$). Dead mangrove again emerged as the highest emitter, averaging 3,020.4 ± 4,780.4 μg m^{-2} h^{-1}, driven largely by one replicate (DM3) with exceptionally elevated emissions. Post-hoc comparisons indicated that CH_4 fluxes at dead mangrove were significantly higher than those at mudflat, rice field, abandoned aquaculture, and healthy mangrove. Marshland exhibited intermediate fluxes (987.4 ± 646.5 μg m^{-2} h^{-1}), while healthy mangrove produced small but consistent emissions (12.0 ± 4.6 μg m^{-2} h^{-1}). Abandoned Aquaculture (0.2 ± 14.4 μg m^{-2} h^{-1}) and rice field (–10.6 ± 45.3 μg m^{-2} h^{-1}) were close to neutral, with the latter showing slight methane uptake. Mudflat acted as a net sink for CH_4 (–206.0 ± 286.7 μg m^{-2} h^{-1}), reinforcing its function as a potential carbon-absorbing system (Figure 8).

The flux results revealed strong contrasts between wetland types, emphasizing how disturbance and ecosystem condition influence carbon gas exchange. Dead mangrove emerged as the most prominent source of both CO_2 and CH_4, with notably high emissions. This pattern mirrors previous findings from degraded mangrove systems, where vegetation dieback and hydrological disruption are known to accelerate organic matter breakdown and greenhouse gas release (Sugiana et al., 2023; Romero-Uribe et al., 2021; Espinosa-Fuentes et al., 2024). Marshland also showed positive fluxes, although with substantial variability among replicates—likely due to fluctuating water levels that create diverse microsites for microbial activity (Gamboa-Cutz et al., 2025; Liu et al., 2017). In contrast, healthy mangrove sites emitted moderate CO_2 and low, consistent CH_4 levels, consistent with stable, undisturbed ecosystems that maintain a balance between carbon

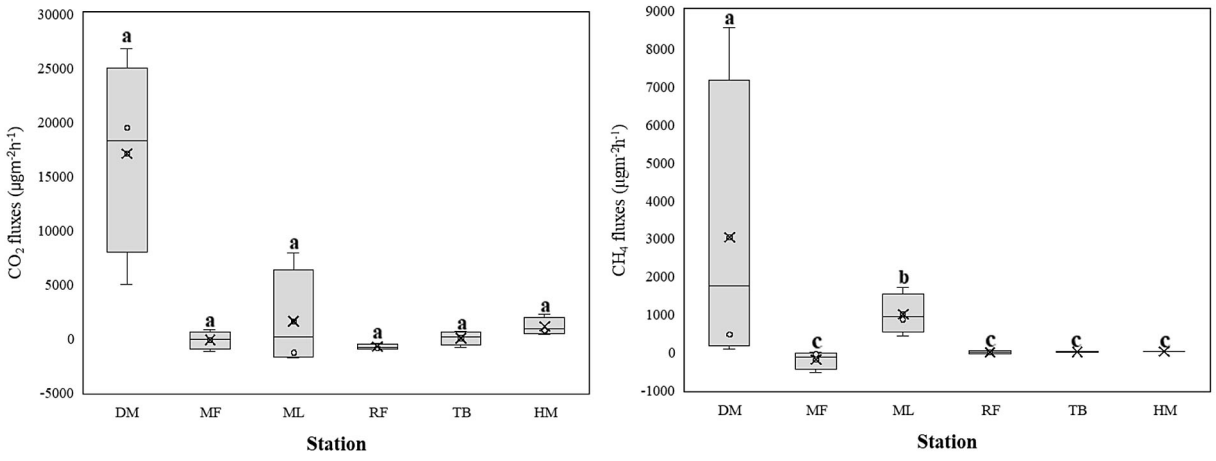

Figure 8. CO_2 fluxes (left) and CH_4 fluxes (right) of each wetland types

uptake and microbial respiration (Donato et al., 2011; Kauffman et al., 2020).

Abandoned aquaculture areas, on the other hand, were nearly neutral in terms of carbon flux, likely due to reduced organic inputs and diminished microbial activity following site abandonment (Castillo et al., 2017; Villa and Bernal, 2018). Meanwhile, both mudflat and rice field acted as net sinks for CO_2 and CH_4, suggesting that oxidation processes or microbial methane consumption (methanotrophy) might be at play. These patterns are in line with prior research on intertidal flats and rice paddies, where such conditions have been shown to suppress emissions or even lead to net uptake of greenhouse gases (Gupta et al., 2021; Basheer et al., 2024; Iram et al., 2021). Altogether, the wetlands in South Bali represent a wide spectrum of carbon dynamics from highly emissive sites like dead mangrove to strong sinks like mudflat and rice field offering insight into the diverse ecological roles these systems play in regional carbon balance (Sugiana et al., 2024; Saunois et al., 2016).

In a broader context, greenhouse gas fluxes measured in this study fall within the wide global range reported for wetlands, although the magnitude and direction vary considerably by site condition. For instance, dead mangrove sites in Bali exhibited far greater CO_2 and CH_4 emissions than nearby healthy mangrove areas, underscoring the impact of disturbance on gas release potential. Conversely, mudflat, rice field, and abandoned aquaculture sites tended to function as net sinks, hinting at their potential contribution to climate mitigation. When compared to global values, the fluxes observed in Bali remain moderate. For example, mangroves in China and Brazil have been shown to emit over 20,000 μg m^{-2} h^{-1} of CO_2, with comparatively low CH_4 levels (Chen et al., 2010; Nobrega et al., 2016). In some extreme cases, disturbed mangroves in the Philippines and mature stands in Australia and Mexico have exceeded 180,000 to 300,000 μg m^{-2} h^{-1} CO_2, with CH_4 fluxes ranging from several hundred to nearly 1.000 μg m^{-2} h^{-1} (Castillo et al., 2017; Kreuzwieser et al., 2003; Romero-Uribe et al., 2021).

Other wetland types also show wide variability. Mangrove systems in Mexico, for instance, have demonstrated near-equilibrium fluxes, with alternating periods of low emission and uptake (Hernández et al., 2020). Rice fields in India and Bangladesh typically report CO_2 emissions between 9.000–10,500 μg m^{-2} h^{-1} and CH_4 fluxes around 400–600 μg m^{-2} h^{-1} (Gupta et al., 2021; Kabir et al., 2014), consistent with regional estimates ranging from 8.000–15,000 μg m^{-2} h^{-1} CO_2 and 400–700 μg m^{-2} h^{-1} CH_4 (Basheer et al., 2024; Sustainability, 2024). Freshwater marshes and swamps can reach even higher emissions, such as 20,000 μg m^{-2} h^{-1} CO_2 and over 1.100 μg m^{-2} h^{-1} CH_4 in Mexico (Marín-Muñiz et al., 2015), and similar magnitudes have been observed in wetland systems in China dominated by Phragmites and Scirpus species (Cao et al., 2020). Peat swamps in Southeast Asia have recorded CO_2 emissions of over 30,000 μg m^{-2} h^{-1} and CH_4 fluxes exceeding 1.200 μg m^{-2} h^{-1} (Adhikari et al., 2020), while high-altitude wetlands on the Qinghai-Tibet Plateau showed lower but still notable fluxes around 14,000 μg m^{-2} h^{-1} CO_2 and 200 μg m^{-2} h^{-1} CH_4 (Liu et al., 2017).

These global comparisons highlight the enormous variability in wetland greenhouse gas fluxes and emphasize the importance of local site characteristics such as vegetation type, hydrology, and land-use history in shaping emission profiles. Subtropical wetlands in Mexico (Espinosa-Fuentes et al., 2024) and abandoned aquaculture systems in the Philippines (Castillo et al., 2017) further demonstrate how disturbance and management strongly influence carbon outcomes. In this context, fluxes observed in Bali may not be exceptional in magnitude, but they are highly representative of the complex dynamics that occur when ecosystems are either degraded or actively managed. The findings reinforce that wetlands can act as either carbon sources or sinks, and that their role in climate regulation depends heavily on their condition, use, and ecological stability.

Carbon fluxes relationship with soil properties

Correlation analysis revealed that CO_2 and CH_4 fluxes were moderately and significantly linked, with a positive association ($r = 0.55^*$, $p < 0.05$) indicating that both gases tended to increase or decrease together across different wetland types. This suggests a degree of shared environmental control or parallel microbial pathways influencing their emissions. CO_2 fluxes also showed a weak positive correlation with total organic carbon ($r = 0.34$, $p > 0.05$) and soil moisture ($r = 0.17$, $p > 0.05$), though these relationships were not statistically significant. On the other hand, CO_2 fluxes were negatively correlated with bulk density ($r = –0.38$, $p > 0.05$) and exhibited a strong

and highly significant negative correlation with pH ($r = –0.67^*$, $p < 0.05$). This implies that lower pH conditions were consistently associated with higher CO_2 emissions, potentially due to increased microbial respiration or inhibited buffering capacity in acidic soils. For CH_4 fluxes, a similar but weaker trend was observed. Weak positive correlations were found with total organic carbon ($r = 0.19$, $p > 0.05$) and water content ($r = 0.09$, $p > 0.05$), while bulk density ($r = –0.28$, $p > 0.05$) and pH ($r = –0.32$, $p > 0.05$) showed weak negative associations. However, none of these relationships reached statistical significance, indicating that CH_4 emissions were more variable and less directly influenced by the measured soil parameters. Overall, these findings suggest that CO_2 fluxes are more strongly governed by underlying soil properties, especially acidity while CH_4 fluxes may depend more on localized factors (Table 3).

The observed relationships between soil carbon fluxes and soil properties illustrate that carbon dioxide and methane emissions are governed by different levels of environmental control. The moderate, statistically significant correlation between CO_2 and CH_4 fluxes suggests a shared influence from processes like anaerobic decomposition and organic matter turnover, even though the extent of their responses varied across wetland types. For CO_2, the strong inverse relationship with soil pH points to a consistent trend where more acidic soils promote higher respiration rates. This is in line with observations from degraded mangrove systems in Mexico and the Philippines, where low pH and redox stress have been shown to stimulate microbial activity (Hernández et al., 2020; Castillo et al., 2017). Although CO_2 fluxes were also weakly and positively linked to total organic carbon and water content, these associations were not statistically significant, suggesting that while carbon substrate and moisture are necessary, they are not always sufficient to drive high emissions—similar to findings from rice field studies where large carbon stocks under flooded conditions did not always correlate with elevated fluxes (Gupta et al., 2021; Kabir et al., 2014). The negative correlation with bulk density indicates that less compacted soils may facilitate microbial access to carbon and gas diffusion, supporting results from freshwater wetlands where porous substrates favored higher gas release (Marín-Muñiz et al., 2015; Cao et al., 2020). In contrast, CH_4 emissions showed only weak, non-significant associations with these same variables, highlighting the more complex controls on methane production. Methanogenesis is highly dependent on specific microbial communities, availability of electron acceptors, and saturation dynamics, factors that are often decoupled from basic soil metrics and better explained through broader ecological and hydrological contexts an interpretation consistent with studies in peat swamps and subtropical wetlands (Nobrega et al., 2016; Espinosa-Fuentes et al., 2024). These findings collectively underscore that CO_2 emissions are more tightly linked to measurable soil properties, particularly acidity, while CH_4 fluxes are shaped by a wider array of biogeochemical and environmental interactions (Romero-Uribe et al., 2021; Basheer et al., 2024).

Table 3. Spearman-rank correlation coefficient between carbon fluxes and soil properties (* correlation significance at $p < 0.05$)

Parameter	Spearman rank coefficient (r)	
	CO_2	CH_4
Total organic carbon (TOC)	0.34	0.19
Bulk density (g cm^{-3})	-0.38	-0.28
Water content (%)	0.17	0.09
pH	-0.67*	-0.32

Climate impact of carbon gases

The evaluation of climate impact based on carbon gas emissions revealed notable differences across the various wetland types. Dead mangrove contributed the strongest warming effect, largely influenced by its high methane output, which carries a much greater global warming potential than carbon dioxide. Marshland also showed a warming effect, though its magnitude was considerably lower than that of dead mangrove. Healthy mangrove sites produced a modest warming signal, while abandoned aquaculture had the lowest warming impact among the emitting wetlands. In contrast, mudflat functioned as the most significant cooling site, driven by negative fluxes of both CO_2 and CH_4, indicating active uptake or suppression of emissions. Rice fields also exhibited a net cooling effect, albeit less pronounced than that observed in mudflats (Table 4). Collectively, these results demonstrate that the net climate role of each wetland type is highly variable, depending on the interplay between CO_2 and CH_4 fluxes and the specific soil and hydrological conditions that govern gas dynamics.

Table 4. Climate impact of carbon gases from each wetland type

Station	Climate impact ($MgCO_{2equivalent}$ $ha^{-1}yr^{-1}$)			Information
	CO_2	CH_4	Total	
DM	1.49 ± 0.97	126.15 ± 199.67	127.65 ± 199.81	Higest warming effect
MF	-0.02 ± 0.09	-8.60 ± 11.97	-8.62 ± 12.06	Higest cooling effect
ML	0.14 ± 0.48	41.24 ± 27.00	41.37 ± 27.45	Still high warming effect
RF	-0.07 ± 0.02	-0.44 ± 1.89	-0.51 ± 1.89	Lowest cooling effect
TB	0.00024 ± 0.0660	0.0079 ± 0.6019	0.00766 ± 0.6677	Lowest warming effect
HM	0.09 ± 0.09	0.50 ± 0.19	0.59 ± 0.21	Low warming effect

The climate impact assessment revealed that wetland types in South Bali differ significantly in their contributions to atmospheric radiative forcing, with some acting as greenhouse gas sources while others function as sinks. Dead mangrove stood out as the most critical emission hotspot, largely driven by elevated methane release a trend consistent with findings from degraded black mangrove ecosystems in Mexico, where seasonal flooding intensified CH_4 output (Romero-Uribe et al., 2021). Marshland also showed a strong warming signal, aligning with patterns observed in subtropical wetlands where high organic content supports continuous emissions (Espinosa-Fuentes et al., 2024). In contrast, healthy mangrove produced only a mild warming effect, highlighting the role of intact ecosystems in stabilizing fluxes, as previously observed in well-preserved mangrove forests in Brazil and China (Nobrega et al., 2016; Chen et al., 2010). Abandoned aquaculture contributed the least warming among the emission-prone sites, like rehabilitated ponds in the Philippines where emissions decline following the cessation of intensive aquaculture (Castillo et al., 2017). Conversely, mudflat served as a significant cooling system, showing net uptake of both CO_2 and CH_4, mirroring conditions in high-altitude wetlands where aerobic soils enable effective greenhouse gas absorption (Liu et al., 2017). Rice fields also exhibited a net cooling effect, although less pronounced, which contrasts with other Asian examples where methane typically dominates emission profiles (Gupta et al., 2021; Kabir et al., 2014). These contrasts demonstrate how hydrology, land-use history, and ecosystem integrity shape the balance between warming and cooling functions.

Beyond identifying the carbon roles of these systems, the findings underscore the urgent need to incorporate wetland conservation and restoration into climate mitigation strategies. Maintaining healthy mangrove stands and restoring degraded areas could significantly reduce methane emissions and improve carbon storage capacity, while avoiding further wetland conversion to aquaculture or agriculture would help preserve their ecological regulation functions (Sugiana et al., 2024). The recognition of mudflats and rice fields as potential cooling systems highlights the value of well-managed coastal and agricultural landscapes in complementing natural ecosystems in climate efforts. This is consistent with global evidence from marshes and peatlands, where water regulation and restoration have demonstrated strong mitigation benefits (Marín-Muñiz et al., 2015; Adhikari et al., 2020). These findings directly support international sustainability goals, particularly SDG 13 (Climate Action), SDG 14 (Life Below Water), and SDG 15 (Life on Land), by showing that climate and biodiversity objectives can be addressed together. Moving forward, research should expand to include seasonal monitoring, integrate nitrous oxide measurements for a fuller greenhouse gas profile, and evaluate restoration outcomes under varying hydrological regimes. Such efforts will be essential to inform policy frameworks that seek to position wetlands as natural climate solutions while supporting biodiversity, sustainable agriculture, and local livelihoods (Basheer et al., 2024).

CONCLUSIONS

This study highlights the diverse carbon dynamics present in South Bali's wetlands, which range from high-emission zones in degraded areas to carbon sinks in environments such as mudflats and rice fields. The clear differences observed among wetland types emphasize the influence of ecosystem integrity, soil characteristics, and historical land use on greenhouse gas fluxes and their

resulting climate effects. While the study was limited to a specific season and timeframe, the consistent trends observed across sites provide strong evidence of distinct emission behaviors tied to wetland condition. Degraded mangroves and disturbed systems emerged as major sources of greenhouse gases, whereas healthier or hydrologically stable wetlands helped buffer or reverse emissions. By combining data on soil properties, gas concentrations, flux rates, and climate implications, this research reveals both the environmental risks associated with ongoing degradation and the climate mitigation potential of strategic conservation and restoration efforts. Actions such as protecting intact mangroves, restoring degraded zones, and improving agricultural wetland management can deliver meaningful climate benefits while supporting local socio-economic resilience. These findings offer important empirical support for integrating wetlands into climate strategies, with implications for regional carbon accounting, coastal resource planning, and the achievement of broader sustainability and biodiversity targets.

Acknowledgement

We would like to thank Universitas Pendidikan Nasional for providing financial support for this research. We also extend our gratitude to Dr. Bruce Campbell for his dedication in reviewing and correcting the English grammar of this manuscript. We declare that there is no conflict of interest in the preparation of this paper.

REFERENCES

1. Adhikari S., Dubey B.K., Lal R. (2020). Greenhouse gas emissions and global warming potential from aquaculture ponds and peatlands: A comparative assessment. *Environmental Science and Pollution Research*, *27*(2), 1234–1247. https://doi.org/10.1007/s11356-019-07015-9
2. Alongi D.M. (2018). Impact of global change on nutrient dynamics in mangrove forests. *Forests*, *9*(10), 596. https://doi.org/10.3390/f9100596
3. Basheer M., Iqbal J., Gupta D.K., Kumar A. (2024). Greenhouse gas emissions from rice-based systems in South Asia: A synthesis. *Sustainability*, *16*(7), 4789. https://doi.org/10.3390/su16074789
4. Cameron C., Hutley L.B., Friess D.A., Munksgaard N.C., Lovelock C.E. (2019). Hydroperiod, soil moisture and bioturbation are critical drivers of greenhouse gas fluxes in Sulawesi mangroves, Indonesia. *Science of the Total Environment*, *654*, 365–377. https://doi.org/10.1016/j.scitotenv.2018.11.123
5. Cao M., Song C., Wang X., Zhang J. (2020). Greenhouse gas fluxes in freshwater swamp wetlands dominated by *Phragmites australis* and *Scirpus triqueter* in northeast China. *Ecological Indicators*, *114*, 106310. https://doi.org/10.1016/j.ecolind.2020.106310
6. Castillo J.A.A., Apan A.A., Maraseni T.N., Salmo S.G. (2017). Soil greenhouse gas fluxes in tropical mangrove forests and land uses on deforested mangrove lands. *Catena*, *159*, 60–69. https://doi.org/10.1016/j.catena.2017.08.005
7. Chen G.C., Tam N.F.Y., Ye Y. (2010). Summer fluxes of CO_2 and CH_4 from mangrove soil in South China. *Science of the Total Environment*, *408*(13), 2761–2767. https://doi.org/10.1016/j.scitotenv.2010.03.008
8. Chen G.C., Ulumuddin Y.I., Pramudji S., Chen S.Y., Chen B., Ye Y., Ou D.Y., Ma Z.Y., Huang H., Wang J.K. (2014). Rich soil carbon and nitrogen but low atmospheric greenhouse gas fluxes from North Sulawesi mangrove swamps in Indonesia. *Science of the Total Environment*, *487*, 91–96. https://doi.org/10.1016/j.scitotenv.2014.03.140
9. Chen L., Zeng C., Tam N.F.Y., Lu W. (2014). Soil greenhouse gas emissions from mangrove forests in China and their global implications. *Biogeosciences*, *11*(19), 5085–5097. https://doi.org/10.5194/bg-11-5085-2014
10. Chen Y., Chen G., Ye Y. (2015). Coastal vegetation invasion increases greenhouse gas emission from wetland soils but also increases soil carbon accumulation. *Science of the Total Environment*, *526*, 19–28. https://doi.org/10.1016/j.scitotenv.2015.04.077
11. Chen G., Chen B., Yu D., Tam N.F., Ye Y., Chen S. (2016). Soil greenhouse gas emissions reduce the contribution of mangrove plants to the atmospheric cooling effect. *Environmental Research Letters*, *11*(12), 124019. https://doi.org/10.1088/1748-9326/11/12/124019
12. Dharmayasa I.G.N.P., Sugiana I.P., Wijana I.M.S., Novanda I.G.A., Aryunisha P.E.P., Wiradana P.A., Mankong P. (2025). Seasonal soil greenhouse gas dynamics: Do mangroves contribute to warming or cooling effect? A case study from Benoa Bay, Indonesia. *Journal of Ecological Engineering*, *26*(8), 187–201.
13. Donato D.C., Kauffman J.B., Murdiyarso D., Kurnianto S., Stidham M., Kanninen M. (2011). Mangroves among the most carbon-rich forests in the tropics. *Nature Geoscience*, *4*(5), 293–297. https://doi.org/10.1038/ngeo1123
14. Espinosa-Fuentes M., Gamboa-Cutz J., González-Valdivia N.A. (2024). Greenhouse gas

emissions from subtropical wetlands under conserved and degraded conditions. *Ecological Engineering*, *199*, 107392. https://doi.org/10.1016/j.ecoleng.2024.107392

15. Gupta D.K., Yadav R.S., Singh S. (2021). Greenhouse gas fluxes from rice fields during monsoon season in India. *Environmental Science and Pollution Research*, *28*(34), 46956–46968. https://doi.org/10.1007/s11356-021-15329-y
16. Hernández M.E., Moreno-Casasola P., Franco-Hernández O. (2020). Soil greenhouse gas fluxes in conserved and degraded mangrove ecosystems of Mexico. *Wetlands Ecology and Management*, *28*(1), 59–74. https://doi.org/10.1007/s11273-019-09687-y
17. IPCC (2021). *Climate change 2021: The physical science basis. Contribution of Working Group I to the Sixth Assessment Report of the Intergovernmental Panel on Climate Change*. Cambridge University Press. https://doi.org/10.1017/9781009157896
18. Kabir M.H., Rahman S.M., Sattar M.A. (2014). Methane and carbon dioxide emissions from rice fields in Bangladesh. *Bangladesh Journal of Environmental Research*, *11*(2), 45–54.
19. Kauffman J.B., Donato D.C. (2012). Protocols for the measurement, monitoring and reporting of structure, biomass and carbon stocks in mangrove forests. *Center for International Forestry Research (CIFOR)*.
20. Kauffman J.B., Arifanti V.B., Schile-Beers L.M., Bernardino A.F., Bhomia R.K., Cifuentes-Jara M.,... Sasmito S.D. (2020). Total ecosystem carbon stocks of mangroves across broad global environmental and physical gradients. *Ecological Monographs*, *90*(2), e01405. https://doi.org/10.1002/ecm.1405
21. Kreuzwieser J., Buchholz J., Rennenberg H. (2003). Emission of methane and nitrous oxide by Australian mangrove ecosystems. *Plant Biology*, *5*(4), 423–431. https://doi.org/10.1055/s-2003-44788
22. Kristensen E., Flindt M.R., Ulomi S., Borges A.V., Abril G., Bouillon S. (2008). Emission of CO_2 and CH_4 to the atmosphere by sediments and open waters in two Tanzanian mangrove forests. *Marine Ecology Progress Series*, *370*, 53–67. https://doi.org/10.3354/meps07642
23. Liu W., Zhang Z., Wan S. (2017). Greenhouse gas fluxes from high-altitude wetlands in China. *Biogeosciences*, *14*(22), 5571–5584. https://doi.org/10.5194/bg-14-5571-2017
24. Marín-Muñiz J.L., Hernández M.E., Moreno-Casasola P. (2015). Greenhouse gas emissions from freshwater marshes in central Veracruz, Mexico. *Ecological Engineering*, *83*, 255–264. https://doi.org/10.1016/j.ecoleng.2015.06.028
25. Nobrega G.N., Ferreira T.O., Otero X.L. (2016). Greenhouse gas emissions from semi-arid mangroves in Brazil. *Estuarine, Coastal and Shelf Science*, *180*, 58–65. https://doi.org/10.1016/j.ecss.2016.06.017
26. Romero-Uribe H.M., López-Portillo J., Reverchon F., Hernández M.E. (2021). Effect of degradation of a black mangrove forest on seasonal greenhouse gas emissions. *Environmental Science and Pollution Research*, *29*(9), 11951–11965. https://doi.org/10.1007/s11356-021-16597-1
27. Rosentreter J.A., Maher D.T., Erler D.V., Murray R., Eyre B.D. (2018). Factors controlling seasonal CO_2 and CH_4 emissions in three tropical mangrove-dominated estuaries. *Estuarine, Coastal and Shelf Science*, *215*, 69–82. https://doi.org/10.1016/j.ecss.2018.10.003
28. Saunois M., Bousquet P., Poulter B., Peregon A., Ciais P., Canadell J.G.,... Zhu Q. (2016). The global methane budget 2000–2012. *Earth System Science Data*, *8*(2), 697–751. https://doi.org/10.5194/essd-8-697-2016
29. Sugiana I.P., Faiqoh E., Adame M.F., Indrawan G.S., Andiani A.A.E., Dewi I.G.A.I.P., Dharmawan I.W.E. (2023). Soil greenhouse gas fluxes to the atmosphere during the wet season across mangrove zones in Benoa Bay, Indonesia. *Asian Journal of Atmospheric Environment*, *17*(1), 13. https://doi.org/10.5572/ajae.2023.17.1.13
30. Sugiana I.P., Prartono T., Rastina R., Koropitan A.F. (2024). Warming effect from soil greenhouse gas emission of each mangrove zone during the dry season in Ngurah Rai Forest Park, Bali, Indonesia. *Environment and Natural Resources Journal*, *22*(5), 449–463. https://doi.org/10.32526/ennrj/22/20240029
31. Thibodeau F.R., Nickerson N.H. (1986). Differential oxidation of mangrove substrate by *Avicennia germinans* and *Rhizophora mangle*. *American Journal of Botany*, *73*(4), 512–516. https://doi.org/10.1002/j.1537-2197.1986.tb12068.x
32. Villa J.A., Bernal B. (2018). Carbon sequestration in wetlands, from science to practice: An overview of the biogeochemical process, measurement methods, and policy framework. *Ecological Engineering*, *114*, 115–128. https://doi.org/10.1016/j.ecoleng.2017.06.037